Theoretical Analysis of Combined Solar System Based on Dual Purpose Solar Collector

Viacheslav Shemelin[1], Nikola Pokorny[1], Tomas Matuska[1] and Borivoj Sourek[1]

[1] University Centre for Energy Efficient Buildings, Czech Technical University in Prague

Abstract

In the present work, the detailed mathematical model of a dual purpose solar collector (DPSC) has been developed and experimentally verified. To demonstrate the application of the DPSC, three buildings with different energy consumption were chosen as case studies and four solar collector systems were compared among one another. The solar yield of the described systems was determined by detailed thermal simulations in TRNSYS using TRNSYS Building environment (TRNBuild) and a detailed theoretical model of DPSC. The results of the modeling indicate that, in the case of combining domestic hot water preparation system and recirculating air heating system based on DPSC, it is possible to achieve a higher solar energy yield compared to a conventional solar domestic hot water preparation system.

Keywords: Solar energy, Dual purpose solar collector, Detailed model, Performance analysis

1. Introduction

Flat plate solar collectors are probably the most fundamental and most studied technology for solar-power domestic hot water systems. Flat plate collector technology has evolved over 60 years. Products on sale today have been proven to be durable and reliable and therefore collectors are considered as a fairly mature technology. However, even if this device has reached good technological level and position on the market, the scientific, and technological world has shown a constant attention to improve the energy performance of the collector. The ways of increasing the energy performance generally can be divided into two categories: the use of new technology, material, component and the combination of already existing solar utilization technologies in one facility (hybrid collector).

The objective of combining two different solar utilization technologies is to make application field for given collector wider and increase potential energy gain from the area occupied by the collector. Known example of such multipurpose collector is e.g. photovoltaic-thermal solar collector combining PV technology and solar thermal collector. The present study is focused on dual fluid solar collector, combining air and liquid solar collector. The idea to combine both types of technology in dual purpose solar collector (DPSC) is not new. It has emerged from the typical situation for moderate and cold climatic zones, where solar radiation is sufficient for preparation of hot water for households needs (50-60 °C) in summer, whereas the output temperatures from solar collectors in winter generally do not reach values higher than 30 °C, however, it can be sufficient, for example, for pre-heating of fresh air. Such integrated design allows to increase an annual energy yield of the solar system and to maximize the operation time, which makes it more cost-effective than the conventional solar water or air systems.

Number of researchers has studied the thermal performance of solar collectors working with two different types of fluids simultaneously. Assari et al. (2011) presented a mathematical model for dual purpose solar collector by effectiveness method. The model was experimentally verified and subsequently was used for the performance analysis of dual purpose solar collector with three different kinds of air channels, such as: rectangular fin, triangular fin and without fin. The results of the modelling indicated that rectangular have better performance compared with the others. Jafari et al. (2011) provided energy and exergy analysis of dual purpose solar collector with triangle air channels. The study showed that dual purpose solar collector has better energy and exergy efficiency that conventional liquid or air collector. Ma et al.(2011) presented experimental and theoretical analysis of the efficiency of dual purpose solar collector with L-shape fins and confirmed that the air flow rate is a key factor for the thermal efficiency. Later Mohajer et al. (2013) conducted an experimental investigation of dual

doi:10.18086/eurosun2018.10.06 Available at http://proceedings.ises.org

purpose solar collector designed by Assari et al. (2011). The experiments showed that the system based on dual purpose solar collectors could be used as for domestic drying system as well as for providing domestic hot water. Arun and Arun (2013) concentrated their research on the utilization of porous medium in the construction of dual purpose solar collector and indicated that utilization of porous medium lead to the increase in the thermal efficiency of the collector. Nematollahi et al. (2014) presented an experimental comparison of single purpose solar system based on liquid collector and dual purpose solar system based on dual purpose solar collector. The results showed the dual purpose system has higher efficiency than single purpose. Venkatesh and Christraj (2015) provided an experimental investigation of multipurpose solar collector system based on combination of water an air collector and confirmed the higher system efficiency compared with the conventional system. As opposed to the previous studies, Ji et al. (2011) provided an analysis of the separate utilization of air and water parts of dual purpose solar collector. In the proposed system building-integrated dual-function solar collector was used to provide space heating in cold winter and water heating in summer. The results showed a decrease in heating load in winter and well performed hot water preparation system in summer season.

In the present study, the detailed theoretical model of DPSC has been developed and experimentally verified. Subsequently the model had been used for annual performance simulation of four different solar systems. To demonstrate the application of the DPSC, three buildings with different energy consumption were chosen as case studies. The distinctive feature of the presented study is a comparison of the different potential applications of dual purpose solar collectors for the buildings with the different heat energy consumption.

2. Detailed Theoretical Model of DPSC

A presented theoretical model of dual purpose solar collector (Type 207) has been developed for TRNSYS simulations based on the previous self-developed models of liquid solar collector (Type 205) and air solar collector (Type 206). More detail information about these models could be found in Shemelin and Matuska, (2017a), Shemelin and Matuska, (2017b) and Shemelin et al. (2017).

2.1 Description of the Model

The presented model is a detailed mathematical model developed for thermal performance simulations of two different solar collector designs. The considered designs of DPSC shown in Fig. 1: Design 1 - It is an absorber pipe upper bond configuration with a single air flow between absorber and a bottom plate; Design 2 - It is an absorber pipe upper bond configuration with a single air flow between an absorber and a transparent insulation.

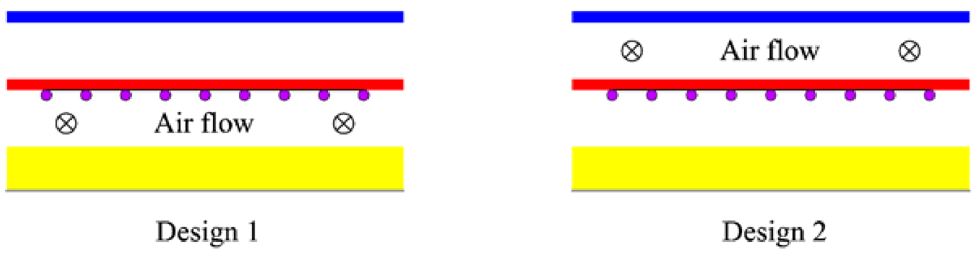

Fig. 1: The considered solar DPSC designs

The DPSC can be specified by a variety of detailed parameters, optical properties of the transparent cover, the absorber and thermophysical properties of main components of the solar collector. Moreover, the transparent cover (glazing, plastic or another transparent insulation structure) and the back thermal insulation are defined by temperature dependent thermal conductance.

The implementation of the model in TRNSYS environment as Type 207 offers the parametric analysis for different construction alternatives for annual solar collector performance in the given solar system application. There is also a possibility to change mathematical models describing the fundamental heat transfer phenomena (natural convection, wind convection, forced convection, etc.) and perform sensitivity analysis for selection of the models.

The presented model does not imply simultaneous work of liquid and air part. It means that DPSC model operates either as a liquid collector or as an air collector, depending on the input – Operating Mode. If Operating Mode is equal to 0, the model operates as a liquid collector; if it is equal to 1, it operates as an air collector.

2.2 Liquid mode (operation of solar liquid collector)

The core of the liquid mode (operation of solar collector for liquid heating) is a mathematical model for solar flat-plate liquid collector solving one-dimensional heat transfer balances. Hottel and Woertz (1942), Hottel and Whillier (1955) and Bliss (1959) developed the simplest assumptions: thermal capacitances are neglected and a single value of collector overall heat loss coefficient is considered. Based on these assumptions and considering that the heat transfer is mainly one-dimensional and predominant in the direction normal to the flow plane, Duffie and Beckman (2013) developed a simplified model (with the electrical analogy) to characterize the solar collector in steady-state conditions. The model solves the energy balance of the solar collector under steady-state conditions according to the principle Hottel-Whillier equation for usable thermal output:

$$\dot{Q}_u = A_{abs} F_R [(\tau\alpha)_n G_t - U(\vartheta_{in} - \vartheta_{amb})] \qquad \text{(eq. 1)}$$

In this equation, A_{abs} is the absorber area (m^2), F_R is the collector heat removal factor (-), τ is the solar transmittance of the collector cover (-), α is the solar absorptance of the absorber (-), G_t is the total solar irradiance (W m^{-2}), U is the overall heat loss coefficient of collector (W m^{-2} K^{-1}), ϑ_{in} is the inlet fluid temperature (K), and ϑ_{amb} is the ambient temperature (K).

The main planes of the collector are cover exterior surface (f_2), cover interior surface (f_1), absorber (*abs*), back insulation interior surface (b_1), back frame exterior surface (b_2), edge insulation interior surface (e_1), and edge frame exterior surface (e_2). A surface temperature is determined for each plane of collector during the calculation procedure. The main collector planes are schematically outlined in Fig. 2.

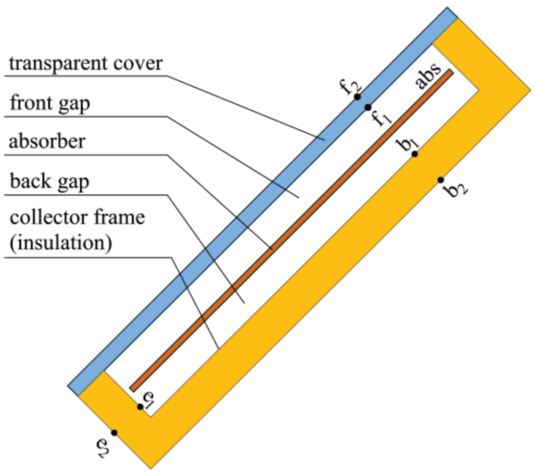

Fig. 2: The main collector planes (surfaces) in the solar collector model

The model in general consists of two parts: external energy balance of absorber (heat transfer from absorber surface to ambient environment) and internal energy balance of absorber (heat transfer from absorber surface into heat transfer fluid). Both external and internal energy balances are mutually dependent. The overall collector heat loss coefficient U (W m^{-2} K^{-1}) as the main output from external balance is one of the inputs for internal balance. On the other side, mean absorber temperature ϑ_{abs} (K) as one of the outputs from internal balance is used as a necessary input for external balance. Iteration loop has been introduced to transfer the results from external balance to starting internal balance and the results from internal balance are put to external balance. Loop iterates as long as the difference between absorber temperatures calculated in two adjacent iteration steps is higher than the required minimum.

2.3 Air mode (operation of solar air collector)

The core of the air mode (operation of solar collector for air heating) is a mathematical model for an air solar collector solving one-dimensional heat transfer balances. This model is a bit more complicated and is described in more details.

To illustrate the procedure for deriving of usable heat gain Q_u (W), efficiency with respect to reference collector area (gross area A_G (m^2)) and output heat transfer fluid temperature ϑ_{out} (K), we derive equations for the most common design of air collector – Design 1 in Fig. 3. The equations for the second design is derived in a similar manner.

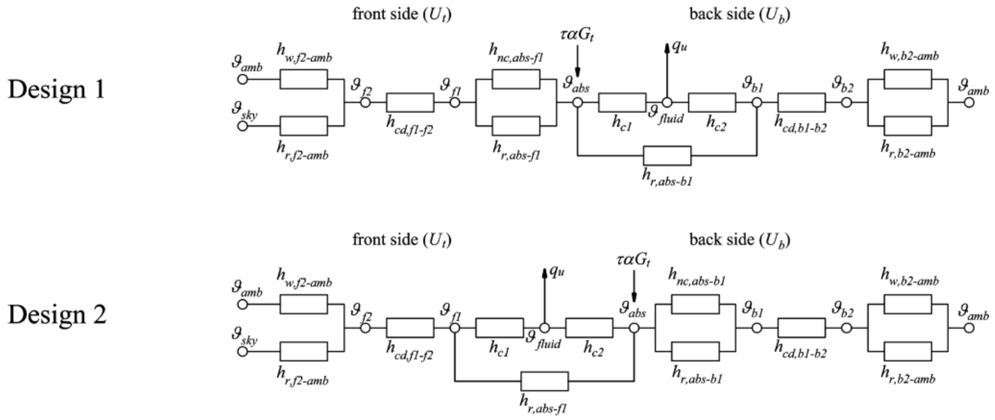

Fig. 3: Thermal network for a solar air collector

Since heat transfer coefficients are temperature dependent, a set of mean temperatures is approximated which allows the heat transfer coefficients to be evaluated as a first guess. Then the surface temperatures are estimated according to a temperature difference between an absorber and an ambient environment uniformly. After that heat transfer coefficients can be calculated and collector heat loss coefficients U_t (W m^{-2} K^{-1}) and U_b (W m^{-2} K^{-1}) can be obtained. Since these coefficients have been calculated for incorrect temperatures, next iteration step follows. From heat transfer coefficients h (W m^{-2} K^{-1}) and heat flows through the front and back sides of a collector the temperature distribution can be obtained by reverse calculation process. To evaluate the new mean temperatures, two different calculation Modes can be used. Mode 1 is based on the Hottel-Whiller-Bliss (eq. 1) general equation for a solar collector performance. Mode 2 uses the heat balances equations for each temperature level and matrix inversion method. The newly calculated mean temperatures are then compared with the initially-guessed temperatures. The iterative process is repeated until all consecutive results of mean temperatures differ by less than 0.01 K.

2.3.1 Mode 1

In steady state, the performance of a solar collector is described by an energy balance that indicates the distribution of incident solar energy into useful energy gain, thermal losses, and optical losses. The solar radiation absorbed by a collector per unit area of absorber A_{abs} (m^2) is equal to the difference between the incident solar radiation and the optical. The thermal energy lost from the collector to the surroundings by conduction, convection, and infrared radiation can be represented as the product of a heat transfer coefficient U (W m^{-2} K^{-1}), times the difference between the mean fluid temperature ϑ_{fluid} (K) and the ambient temperature ϑ_{amb} (K):

$$\dot{Q}_u = A_{abs}F'\left[(\tau\alpha)_n G_t - U\left(\vartheta_{fluid} - \vartheta_{amb}\right)\right] \qquad \text{(eq. 2)}$$

The problem with this equation is that the overall heat loss coefficient U (W m^{-2} K^{-1}) and the collector efficiency factor F' (-) is difficult to calculate. The algebra is somewhat tedious and only results of deriving F' (-) and U (W m^{-2} K^{-1}) are presented.

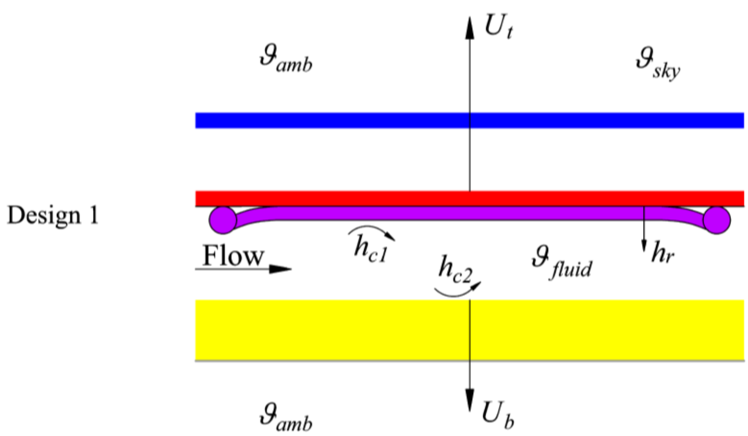

Fig. 4: Schematic view of solar air collector with single air flow between an absorber and a bottom plate

$$U = U_t + U_b \tag{eq. 3}$$

$$F' = \frac{1}{1+\frac{U}{h_{c1}+\frac{1}{\frac{1}{h_{c2}}+\frac{1}{h_{r,abs-b1}}}}} \tag{eq. 4}$$

Design 2

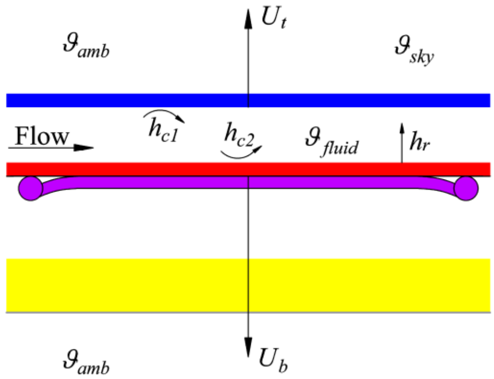

Fig. 5: Schematic view of solar air collector with single air flow between absorber and transparent insulation

$$U = \frac{(U_t+U_b)(h_{c1}h_{c2}+h_{r,abs-f1}h_{c1}+h_{r,abs-f1}h_{c2})+U_bU_t(h_{c1}+h_{c2})}{h_{c1}h_{r,abs-f1}+h_{c2}U_t+h_{c2}h_{r,abs-f1}+h_{c1}h_{c2}} \tag{eq. 5}$$

$$F' = \frac{h_{r,abs-f1}h_{c1}+h_{c2}U_t+h_{c2}h_{r,abs-f1}+h_{c1}h_{c2}}{(U_t+h_{r,abs-f1}+h_{c1})(U_b+h_{c2}+h_{r,abs-f1})-h_{r,abs-f1}^2} \tag{eq. 6}$$

After that the collector flow factor F'' (-), the collector heat removal factor F_R (-), the useful energy gain, and the outlet temperature can be obtained. Since these values have been calculated for first estimates of temperatures, next iteration step should follow. To calculate heat transfer coefficients at main surfaces of solar collector and to assess the overall collector heat loss coefficient U (W m^{-2} K^{-1}) in the next iteration step, the absorber temperature, the mean fluid temperature, and the temperature distribution should be derived.

2.3.2 Mode 2

Mode 2 operates in a principally different manner. The core of the Mode 2 is a set of heat balance equations obtained from the thermal network at the points:

$$\vartheta_{f1}:\ \ h_{r,f2-amb}(\vartheta_{f2}-\vartheta_{sky}) + h_{w,f2-amb}(\vartheta_{f2}-\vartheta_{amb}) = h_{cd,f1-f2}(\vartheta_{f1}-\vartheta_{f2}) \tag{eq. 7}$$

$$\vartheta_{f2}:\ \ h_{cd,f1-f2}(\vartheta_{f1}-\vartheta_{f2}) = h_{r,abs-f1}(\vartheta_{abs}-\vartheta_{f1}) + h_{nc}(\vartheta_{abs}-\vartheta_{f1}) \tag{eq. 8}$$

$$\vartheta_{abs}:\ \ \tau\alpha G = (h_{r,abs-f1}+h_{nc})(\vartheta_{abs}-\vartheta_{f1}) + h_{r,abs-b1}(\vartheta_{abs}-\vartheta_{b1}) + h_{c1}(\vartheta_{abs}-\vartheta_{fluid}) \tag{eq. 9}$$

$$\vartheta_{fluid}:\ h_{c1}(\vartheta_{abs}-\vartheta_{fluid}) = h_{c2}(\vartheta_{fluid}-\vartheta_{b2}) + \frac{2mc_f}{S}(\vartheta_{fluid}-\vartheta_{in}) \tag{eq. 10}$$

$$\vartheta_{b2}:\ h_{r,abs-b1}(\vartheta_{abs}-\vartheta_{b1}) + h_{c2}(\vartheta_{fluid}-\vartheta_{b1}) = h_{cd,b1-b2}(\vartheta_{b1}-\vartheta_{b2}) \tag{eq. 11}$$

$$\vartheta_{b1}:\ h_{cd,b1-b2}(\vartheta_{b1}-\vartheta_{b2}) = h_{r,b2-amb}(\vartheta_{b2}-\vartheta_{amb}) + h_{w,b2-amb}(\vartheta_{b2}-\vartheta_{amb}) \tag{eq. 12}$$

By rearranging, we obtain a system of linear equations in the matrix form:

$$\begin{bmatrix} h_{r,f2-amb}+h_{w,f2-amb}+h_{cd,f1-f2} & -h_{cd,f1-f2} & 0 & 0 & 0 & 0 \\ -h_{cd,f1-f2} & h_{cd,f1-f2}+h_{r,abs-f1}+h_{nc} & -h_{r,abs-f1}-h_{nc} & 0 & 0 & 0 \\ 0 & -h_{r,abs-f1}-h_{nc} & h_{r,abs-f1}+h_{nc}+h_{r,abs-b1}+h_{c1} & -h_{c1} & -h_{r,abs-b1} & 0 \\ 0 & 0 & h_{c1} & -h_{c1}-h_{c2}-\frac{2mc_f}{S} & h_{c2} & 0 \\ 0 & 0 & h_{r,abs-b1} & h_{c2} & -h_{r,abs-b1}-h_{c2}-h_{cd,b1-b2} & h_{cd,b1-b2} \\ 0 & 0 & 0 & 0 & h_{cd,b1-b2} & h_{r,b2-amb}+h_{w,b2-amb}+h_{cd,b1-b2} \end{bmatrix} \begin{bmatrix} \vartheta_{f2} \\ \vartheta_{f1} \\ \vartheta_{abs} \\ \vartheta_{fluid} \\ \vartheta_{b1} \\ \vartheta_{b2} \end{bmatrix} = \begin{bmatrix} h_{r,f2-amb}\vartheta_{sky}+h_{w,f2-amb}\vartheta_{amb} \\ 0 \\ \tau\alpha G \\ \frac{2mc_f}{S}\vartheta_{in} \\ 0 \\ h_{r,b2-amb}\vartheta_{amb}+h_{w,b2-amb}\vartheta_{amb} \end{bmatrix} \tag{eq. 13}$$

In general, the above matrices may be displayed as

$$[A][T] = [B] \qquad \text{(eq. 14)}$$

The mean temperature vector may be determined by matrix inversion as

$$[T] = [A]^{-1}[B] \qquad \text{(eq. 15)}$$

Since the mean temperature vector is calculated, the outlet fluid temperature and the useful energy gain can be determined.

2.4 Model verification

The model has been experimentally validated on prototype of DPSC (design 1) in the frame of solar collectors testing according to the European standard EN ISO 9806 in the accredited Solar Laboratory of Czech Technical University in Prague. The verification of liquid and air parts has been conducted separately. The prototype of DPSC has been built from the experimental solar water collector by adjusting the interior air gap (Fig. 6). The detailed parameters of the produced prototype are listed in the Tab. 1. If the operation mode is liquid heating, water flows in the copper tubes, and the air channels are closed at inlet and outlet. On the other side, the inlet and outlet of water pipes are closed in air heating mode.

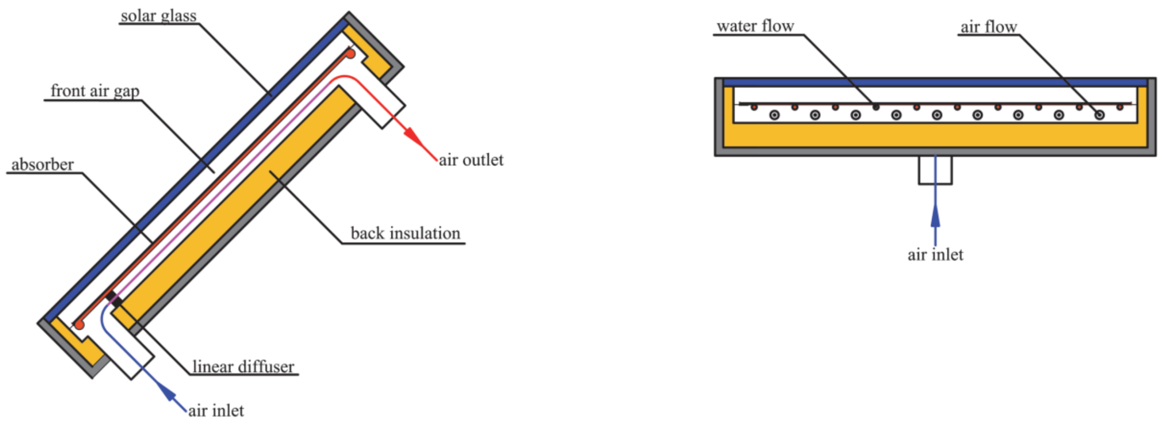

Fig. 6 Design of prototype of DPSC collector

Tab. 1: Design parameters of the DPSC used in the analysis

Collector parameter	Value	Collector parameter	Value
Dimensions (W/L/H)	1 x 1.6 x 0.087 m	Absorber emissivity	0.05
Area (gross, aperture, absorber)	1.6 m^2, 1.52 m^2, 1.49 m^2	Header pipe	Cu 22 x 1 mm
Cover material	Solar glass 4 mm	Number of riser tubes	10
Front air gap thickness	30 mm	Distance between riser pipes	100 mm
Absorber material	Aluminium 0.4 mm	Air flow channel	20 mm
Cover transmittance	0.92	Back insulation thickness	30 mm
Absorber absorptance	0.95	Insulation material	Rockwool

Fig. 7 and Fig. 8 show experimentally evaluated efficiency points and theoretically modelled efficiency characteristics both in liquid and air operation modes. Experimental data points of solar collector efficiency are coupled with combined standard uncertainty bars in the graphs. The uncertainty analysis has been provided based on methodology published in Mathioulakis et al. (1999) and Müller-Schöll and Frei (2000). The theoretical calculation of efficiency characteristic by the model is subjected to the uncertainty of real collector parameters which are used as inputs for the model. Therefore, the results of theoretical calculation could be presented as two delimiting curves where the collector efficiency values can be found in reality. It is evident from the results that simulated efficiency characteristics fit the measurements relatively well, which gives confidence in the developed model. More information about model verification and uncertainty analysis can be found in Shemelin et al. (2017).

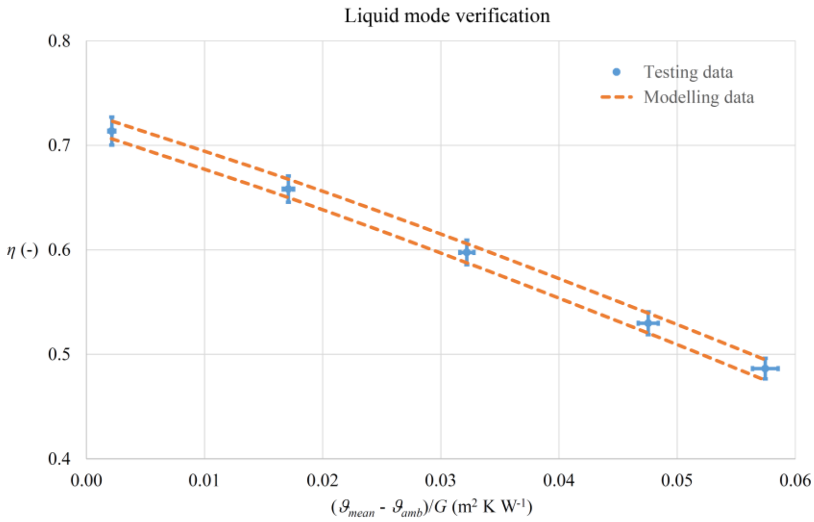

Fig. 7: Mathematical model verification - liquid heating mode

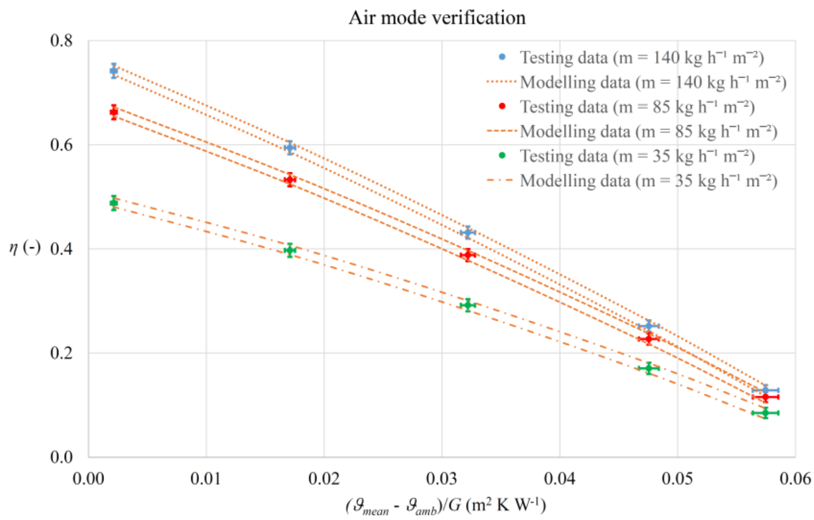

Fig. 8: Mathematical model verification - air heating mode

3. Hybrid solar energy system

To evaluate the energy performance of DPSC system, system annual solar yield has been analyzed for a specific site and under the specific conditions. Three single family houses with the same heated floor area of 246 m^2 and with different energy consumption were considered as case studies for comparative analysis (Fig. 9). The detailed buildings parameters are listed in the Tab. 2.

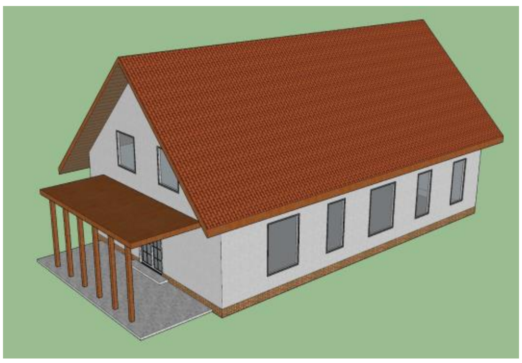

Fig. 9: Three-dimensional geometry of the considered buildings

Tab. 2: The buildings key values

Key Values	**Building A**	**Building B**	**Building C**
General data			
Occupancy	4 persons		
City location	Prague		
Climate data source	Meteonorm		
Annual total horizontal radiation	998 kWh m^{-2}		
Mean annual temperature	8.9 °C		
Set point temperature (day/night)	20 °C / 20 °C		
Ventilation air flow rate	100 m^3 h^{-1}		
Internal gains (occupants + equipments)	2 W m^{-2}		
Heating season	234 days		
Building geometry data			
Gross Floor Area	286 m^2		
Heated Floor Area	246 m^2		
Ventilated Volume	607.1 m^3		
Specific Annual Demands			
Hot water generation	12 kWh m^{-2}	12 kWh m^{-2}	12 kWh m^{-2}
Net heating energy	38 kWh m^{-2}	79 kWh m^{-2}	112 kWh m^{-2}
Net cooling energy	7 kWh m^{-2}	2 kWh m^{-2}	0 kWh m^{-2}

Four different solar energy systems were compared in the analysis. The reference system (RS) is a standard solar domestic hot water system with a solar fraction 60 % based on conventional flat-plate liquid collectors with the following parameters: optical efficiency 0.81, linear heat loss coefficient 3.58 W m^{-2} K^{-1}, quadratic heat loss coefficient 0.0045 W m^{-2} K^{-2}, incidence angle modifier IAM_{50} = 0.92. The detailed parameters of the reference system are listed in the Tab. 3.

Tab. 3: Solar domestic hot water system parameters and operating conditions (RC, V1, V2 and V3)

Parameter	**Description**
Collector orientation	South, 45°
Collector area	4.8 m^2 (gross area)
Collector mass flow rate	50 l h^{-1} m^{-2}
Heat transfer medium	Propylene Glycol
Pump control	Pump switching on/off temperature difference collector-storage 8 K / 2 K
Piping	Supply and return pipes are located in the internal and external environments: 10 m each, DN 16 with 25 mm thermal insulation (λ = 0.04 W m^{-2} K^{-1}).
Heat exchanger	Smooth tube heat exchanger with *UA* = 400 W K^{-1} (±15%) for 42 °C / 40 °C (inlet temperature/tank storage temperature)
Tank storage	Volume: 200 l, heat loss: 1.4 kWh day^{-1}, height/diameter ratio: 2.5
Cold water temperature	10 °C
Building interior temperature	20 °C
Hot water consumption	160 l day^{-1} (7.00 : 65 l; 12.00 : 30 l; 19.00 : 65 l), hot water temperature 55 °C

The first alternative system (V1) is based on DPSC which operates from May to September in a liquid mode for hot water preparation (as the reference system) and the rest of the year (winter) for pre-heating of fresh air before the heat recovery unit. In the air mode, the fresh air is led through the collector and then optionally heated in the heat recovery unit. In the case of insufficient sunlight (clouded sky or night time), the air bypasses the collector.

The second system (V2) has the same configuration as the first alternative (V1) with the exception that the collector is installed at output of the heat recovery unit. In the air heating mode, the fresh air is firstly preheated in the heat recovery unit and then optionally is led through the collector. The preheated air is led through the collector only in the case if the collector has a potential to heat the air, otherwise the preheated air bypasses the collector.

The third system (V3) differs from the previous two systems - the DPSC operates from May to September in a liquid mode for hot water preparation (as the reference system) and in the rest of the year operates as solar air collector in direct recirculating air heating system. In the air heating mode, the circulating air sucked from the rooms is heated in the collector and is led to the building. The fresh air, after preheating in the heat recovery unit, is mixed with the circulation air and only after is brought into the living rooms. On cloudy days and at night the circulation air does not flow through the collector.

The design parameters of the DPSC collector which were used for simulation of all alternative systems (V1, V2, and V3) are the same as the prototype DPSC and are listed in the Tab. 1. The solar domestic hot water system parameters in the liquid mode is are same as for reference system and are listed in the Tab. 3. The air heating mode system parameters are shown in the Tab. 4.

Tab. 4: Air heating mode (V1, V2, and V3)

Parameter	V1	V2	V3
Collector orientation	South, 45°		
Collector area	4.8 m^2		
Reference area	Gross area		
Set point temperature	22 °C		
Function	Fresh air preheating (before h. r. u.)	Fresh air preheating (after h. r. u.)	Direct air heating (circulating air)
Air flow rate	100 $m^3 h^{-1}$	100 $m^3 h^{-1}$	400 $m^3 h^{-1}$

The overview of the compared solar systems is presented in Fig. 10.

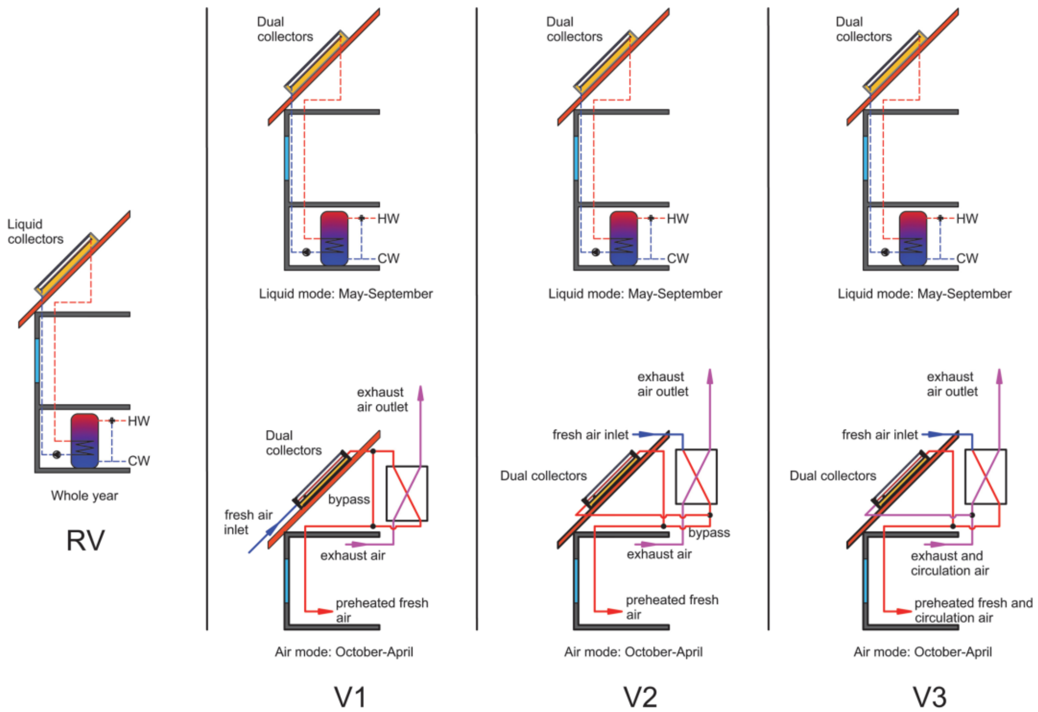

Fig. 10: Considered solar collector system variants

4. Results and discussion

To demonstrate the application of the DPSC, three buildings with the different energy consumption (Building A, B, and C) were chosen as case studies and four solar collector systems (RV, V1, V2, and V3) were compared. The solar yield of the described systems was determined by detailed thermal simulations in TRNSYS, using TRNSYS Building environment (TRNBuild) and detailed theoretical model of DPSC.

The results are shown in Fig.11 and in Tab. 5. Firstly, the results of the simulation indicate that DPSC design allows increasing the annual energy yield of the solar system. It can be explained by the fact, that in winter the intensity of solar radiation is not sufficient to heat the heat transfer liquid by 8 °C (pump switching temperature), but on the other hand, it is sufficient to heat the fresh or circulation air. Besides, it can be seen that the higher building heat energy consumption is respectively correlated to the higher solar energy yield of compared systems. It means that DPSC in air mode not only reduces the ventilation heat loss but also contributes to a reduction of the overall heating demand.

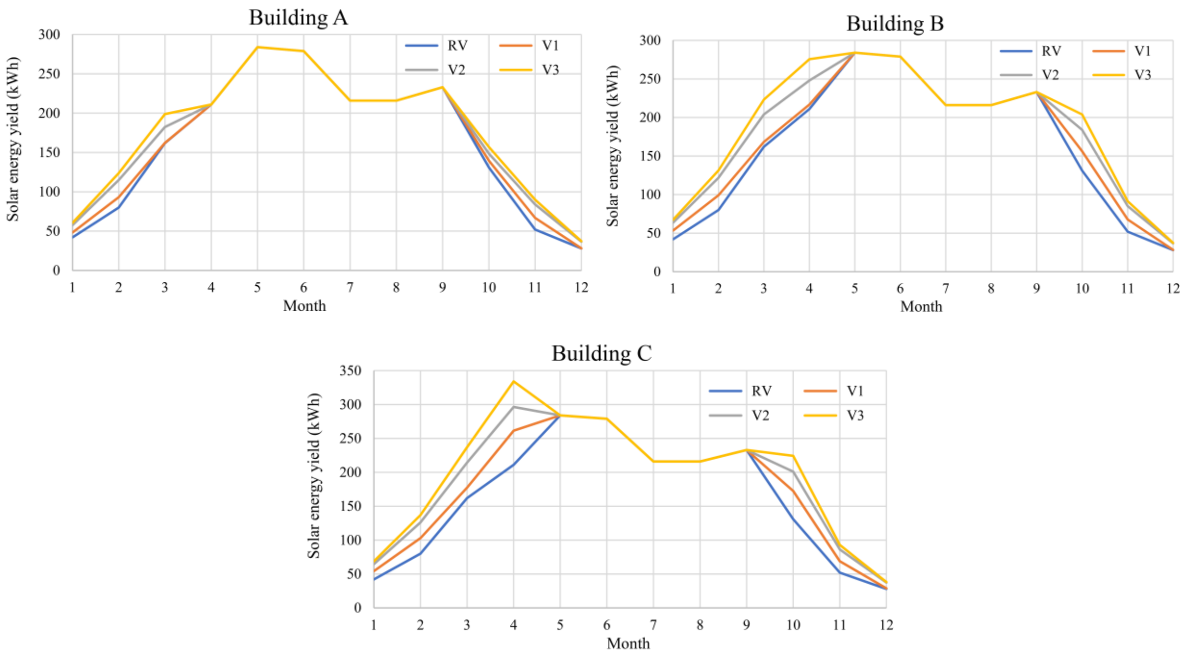

Fig. 11: Annual performance of the compared solar systems

Tab. 5: Annual solar energy yield of solar system alternatives (kWh m^{-2})

Building	RS	V1	V2	V3
Building A (annual heat demand 38 kWh m^{-2})	403	412	430	439
Building B (annual heat demand 79 kWh m^{-2})	403	420	452	470
Building C (annual heat demand 112 kWh m^{-2})	403	436	470	492

Secondly, it can be observed that the third alternative system V3 shows the highest annual solar energy yield among the compared systems. This result is a consequence of higher efficiency of DPSC (air mode) in the system V3. The efficiency of air part of DPSC depends on a number of parameters and the mode dominant of these is collector air flow rate (Fig. 8). Since in the case of the first and of the second alternative systems the collector air flow rate is limited by the ventilation air flow rate 100 m^3 h^{-1}, in the case of the third alternative system can be increased to 400 m^3 h^{-1}.

The combination of DPSC system with heat recovery from the exhaust air reduces the effectively possible heating energy savings by the DPSC collector. The DPSC and heat recovery system compete and the potential savings are limited in total.

In the case of the first alternative system V1, the performance of the heat recovery unit is limited because the air temperature after DPSC is higher than the outdoor temperature. Moreover, if the fresh air temperature after DPSC is higher than 18 °C, the fresh air bypasses the heat recovery unit and flows directly to the building.

If the collector is placed behind the heat recovery unit to provide additional temperature rises of the room inlet air, the collector system is energetically more favourable (system V2). Nevertheless, the efficiency of DPSC is limited because the air temperature after the heat recovery unit is higher than the outdoor temperature and consequently the solar collector thermal losses are higher compared to system V1.

5. Conclusion

Detailed mathematical model of DPSC has been developed and validated by the experiment for the collector in liquid and air mode. Subsequently, the comprehensive analysis of different solar systems based on DPSC for three buildings with the different energy consumption has been provided.

Based on the simulation runs using practical design data, the following can be concluded:

- All compared alternative systems based on DPSC have shown the higher annular solar energy yield than the reference system based on liquid solar collectors.
- The combination of DPSC system with heat recovery from the exhaust air reduces the effectively possible heating energy savings.
- The third alternative system V3 shows the highest annual solar energy yield among the compared systems.

Based on the promising simulation results now it is possible to proceed to parametric analyses and optimization of the design of DPSC towards the higher performance.

6. Acknowledgment

This work has been supported by the Ministry of Education, Youth and Sports within National Sustainability Programme I, project No. LO1605.

7. References

AK, A.V., Arun, P., 2013. Simulation studies on porous medium integrated dual purpose solar collector. Int. J. Renew. Energy Res. 3, 114–120.

Assari, M.R., Basirat Tabrizi, H., Jafari, I., 2011. Experimental and theoretical investigation of dual purpose solar collector. Sol. Energy 85, 601–608. https://doi.org/10.1016/j.solener.2011.01.006

Bliss Jr., R.W., 1959. The derivations of several “Plate-efficiency factors” useful in the design of flat-plate solar heat collectors. Sol. Energy 3, 55–64. https://doi.org/10.1016/0038-092X(59)90006-4

Duffie, J.A., Beckman, W.A., 2013. Solar engineering of thermal processes. John Wiley & Sons.

Hottel, H., Whillier, A., 1955. Evaluation of flat-plate solar collector performance. Trans. Conf. Use Sol. Energy; 3, 74–104.

Hottel, H., Woertz, B., 1942. Performance of flat-plate solar-heat collectors. Trans. ASME (Am. Soc. Mech. Eng.); (United States) 64, 91–104.

Jafari, I., Ershadi, A., Najafpour, E., Hedayat, N., 2011. Energy and exergy analysis of dual purpose solar collector. Acad Sci Technol 81, 259–261.

Ji, J., Luo, C., Chow, T.-T., Sun, W., He, W., 2011. Thermal characteristics of a building-integrated dual-function solar collector in water heating mode with natural circulation. Energy 36, 566–574. https://doi.org/10.1016/j.energy.2010.10.004

Ma, J., Sun, W., Ji, J., Zhang, Y., Zhang, A., Fan, W., 2011. Experimental and theoretical study of the efficiency of a dual-function solar collector. Appl. Therm. Eng. 31, 1751–1756. https://doi.org/10.1016/j.applthermaleng.2011.02.019

Mathioulakis, E., Voropoulos, K., Belessiotis, V., 1999. Assessment of uncertainty in solar collector modeling and testing. Sol. Energy 66, 337–347. https://doi.org/10.1016/S0038-092X(99)00034-1

Mohajer, A., Nematollahi, O., Joybari, M.M., Hashemi, S.A., Assari, M.R., 2013. Experimental investigation of a Hybrid Solar Drier and Water Heater System. Energy Convers. Manag. 76, 935–944. https://doi.org/10.1016/j.enconman.2013.08.047

Müller-Schöll, C., Frei, U., 2000. Uncertainty analyses in solar collector measurement. Tc 1000, 7.

Nematollahi, O., Alamdari, P., Assari, M.R., 2014. Experimental investigation of a dual purpose solar heating system. Energy Convers. Manag. 78, 359–366. https://doi.org/10.1016/j.enconman.2013.10.046

Shemelin, V., Matuska, T., 2017a. TRNSYS type 205-Model of glazed solar liquid collector based on detailed construction parameters and energy balance. Available at: http://users.fs.cvut.cz/tomas.matuska/?page_id=582 [Accessed November 20, 2018].

Shemelin, V., Matuska, T., 2017b. TRNSYS type 206-Model of glazed solar air collector based on detailed construction parameters and energy balance. Available at: http://users.fs.cvut.cz/tomas.matuska/?page_id=951 [Accessed November 20, 2018].

Shemelin, V., Matuska, T., Sourek, B., 2017. TRNSYS type 207 – Model of dual solar air-liquid collector based on detailed construction parameteres and energy balance. Available at: http://users.fs.cvut.cz/tomas.matuska/?page_id=965 [Accessed November 20, 2018]

Venkatesh, R., Christraj, W., 2015. Experimental Investigation of Multipurpose Solar Heating System. J. Energy Eng. 141, 04014009. https://doi.org/10.1061/(ASCE)EY.1943-7897.0000166.